Bulletin of Engineering Geology and the Environment (2019) 78:5991–6002
https://doi.org/10.1007/s10064-019-01500-7

ORIGINAL PAPER

Damage evolution behavior and constitutive model of sandstone subjected to chemical corrosion

Yun Lin[1,2] · Keping Zhou[1] · Feng Gao[1] · Jielin Li[1]

Received: 18 October 2018 / Accepted: 7 March 2019 / Published online: 28 March 2019

Abstract

Chemical corrosion has significant impact on the properties of rock materials. To investigate the effect of chemical corrosion on the porosity and mechanical properties of sandstones, the nuclear magnetic resonance (NMR) technique was used for the measurement of porosity. Uniaxial compression tests were then conducted for rock specimens treated with chemical corrosions. The test results showed that, compared with the rock specimens in their natural state, after chemical corrosions, the porosity increased, the uniaxial compressive strength and elastic modulus of sandstone both decreased, but the corresponding peak strain increased. A chemical damage variable derived from the change of porosity and the effective bearing area of rock samples was proposed. Based on the chemical damage variable, the corrosion order of different chemical solutions on sandstone was obtained as H_2SO_4 > NaOH > distilled water. The mechanism of chemical corrosion was also explored based on water-rock reactions. Finally, by introducing the compaction coefficient, an improved statistical damage constitutive model was established to describe the damage evolution of the sandstones treated with different chemical corrosions.

Keywords Chemical corrosion · Porosity · Chemical damage variable · Compaction coefficient · Damage constitutive model

Introduction

Water is one of the most active factors in rock engineering applications (Lu et al. 2016), such as in oil and gas extraction, mining engineering, nuclear waste repositories, geothermal heat extraction and carbon dioxide geological sequestration (Han et al. 2016; Han et al. 2017; Hu et al. 2012; Tang et al. 2002). The interaction between water and rocks in these applications could have significant impacts on the mechanical behaviors and properties of the rock. In particular, chemical corrosion due to dissolution of minerals in water solution can affect significantly the deformability and strength of the rock, hence the stability of rock excavation structures. Therefore, the study of the damage evolution mechanisms of rock in different chemical environments is one of the most fundamental research topics in rock engineering.

✉ Keping Zhou
kpzhou@vip.163.com

[1] School of Resource and Safety Engineering, Central South University, Changsha 410083, Hunan, China

[2] School of Civil, Environmental and Mining Engineering, University of Adelaide, Adelaide, SA 5005, Australia

It is obvious that rock becomes weaker due to chemical corrosion, reflected in the reduction in elastic modules and strength, such as uniaxial compression strength (UCS). A significant amount of researches in this topic have been published (Feng et al. 2004; Han et al. 2017; Hu et al. 2012; Li et al. 2003; Ni et al. 2016; Qiao et al. 2016). These researches mainly focus on the influence of chemical solutions on the macroscopic mechanical behaviors of rocks and different chemical damage variables. For example, Li et al. (2003) defined their chemical damage variable according to the effective bearing area of cementing materials. Chaki et al. (2008) and Han et al. (2016) established their chemical damage variable based on the increment of porosity inside the rock. Ni et al. (2016) calculated porosity based on P wave velocity to define their chemical damage variable, and analyzed the relationship between the deterioration of mechanical properties of rock and different chemical solutions. Li et al. (2018) experimentally investigated the micro-damage evolution of chemically corroded limestone. These results are of great significance to the understanding of the deterioration of mechanical properties of rocks due to chemical corrosion.

The damage, deformation and failure process of rock can be well reflected by damage constitutive models (Xu et al. 2017). Thus, a reasonable damage constitutive model of rock

is crucial in the design and stability analysis of rock engineering (Zhao et al. 2016). In the literature, many constitutive models have been established based on theoretical and experimental approaches (Darabi et al. 2012; Deng and Gu 2011; Li and Tang 2015; Li et al. 2016a; Li et al. 2012; Pourhosseini and Shabanimashcool 2014; Qu et al. 2018; Wang et al. 2007; Xu et al. 2017; Xu and Karakus 2018). The deformation and failure characteristics of rock under chemical corrosion are different from that of rock under natural state or other external factors (freeze-thaw, high temperature). In recent years, study of the constitutive relationship of rocks under the condition of chemical corrosion has been the focus of many scholars. For example, Jiang and Wen (2011) used the axial strain to describe the strength of micro-units, and then established a damage constitutive model of sandstone during corrosion by acid mine drainage (AMD). Miao et al. (2018) proposed a new chemical damage variable in terms of primary and secondary porosity, and established a damage constitutive model of rock under the condition of acidic solution corrosion. Li et al. (2018) proposed a damage model of limestone under cyclic loading and acidic solution corrosion. All of the results are important for investigating the mechanical behavior of rocks subjected to hydro-chemical corrosion, and this research has received more attention in the past few decades.

Though the study on the topic has received some attention in the past few decades, published research is still very limited, and their results are far from providing a good understanding of the characteristics of rock deformation and destruction under the corrosion of different chemical solutions. Moreover, the damage mechanisms have also not been well investigated. Particularly, the definition of chemical damage variable was various in the above literatures. All of these address a need to establish a new damage constitutive model of rocks under the coupled effect of different chemical corrosions and loading.

To investigate the deterioration of mechanical properties of rock treated with different chemical solutions, nuclear magnetic resonance (NMR) technology was used to measure rock porosity of sandstone specimens, and a series of uniaxial compression tests were carried out to determine the UCS and the elastic modulus of treated specimens. A new chemical damage variable was established in terms of the change of porosity, and an improved statistical damage constitutive model of sandstone at different degrees of chemical corrosion was then proposed.

Materials and experimental methods

Materials preparation

The rock used in this study is a fine-grained sandstone collected from a deep underground mine in Hunan Province, China. The sandstone is unweathered. In order to ensure the reliability of test results, all samples were cored from the same sandstone block with no visible geological weakness. The mineral composition of the rock was determined by X-ray diffraction (XRD) technique. The result showed that the sandstone is mainly composed of 75% quartz, 12% feldspar, 7% mica, 3% calcite and 2% chlorite. Some other mineral compositions, like clay minerals, are less than 1% by weight.

Cylindrical specimens were prepared according to ISRM standards (Bieniawski and Bernede 1979) with the diameter of 50 ± 1 mm and the height of 100 ± 1 mm. Both end surfaces of specimens were carefully ground to ensure the roughness was less than 0.2 mm (Li et al. 2016b; Yang et al. 2017) and the non-parallelism was within ± 0.1%. All samples were intact and uniform. In addition, to eliminate the influence of rock heterogeneity and anisotropy on rock mechanics properties, samples with macroscopic joint fissures were excluded. Furthermore, specimens were screened for anomalies where those having outlier values of longitudinal wave velocity (LWV) and abnormal NMR microstructures were also excluded for further testing. The mean porosity, density and LWV of retained specimens were 5.06%, 2.29 g/cm^3 and 2260 m/s, respectively.

In our experiments, three aqueous chemical solutions with varying pH values were prepared: an acidic solution with 0.01 mol/L H_2SO_4 (pH = 2), distilled water (pH = 7) and an alkaline solution with 0.01 mol/L NaOH (pH = 12). Taking into account the natural state of the sandstone, there are four test groups (labeled as A, B, C and D) and each group has four specimens (labeled as 1, 2, 3 and 4). The specimens from groups A, B and C were treated in acidic solution, distilled water and alkaline solution, respectively. Group D represents the group of specimens in their natural state.

Experimental setup and test procedure

The porosity of the sandstones was measured or obtained by an AniMR-150 NMR imaging system (Liu et al. 2017; Zhou et al. 2015; Zhou et al. 2018; Zhou et al. 2016). The strength of the main magnetic field is 0.51 T. The gradient field in three directions is 0. 03 T/m. The proton resonance frequency is 21.7 MHz, and the radio frequency pulse is in the range of 1.0–49.9 MHz. The uniformity of the magnet is 12.0 ppm. Note that the temperature of the magnet should be controlled to 25–35 °C to ensure the reliability of measured results.

The uniaxial compression tests for all specimens were conducted on an Instron 1346 material testing machine with a maximum load of 2000 KN. The experiment used the axial displacement control, and the loading rate was a constant of 0.15 mm/min. During testing, the axial load and displacement were recorded. In this study, the UCS of the specimen was calculated based on the peak load when the specimen failed,

and the elastic modulus was the slope of the major linear segment in the stress–strain curve.

All specimens were prepared and tested following these steps: (1) Specimens were prepared and screened for anomalies in preparation quality, LWV and NMR microstructure; (2) Specimens were then submerged in chemical solutions; (3) Specimens were tested for porosity every 10 days using NMR technique until the porosity became relatively constant; (4) Uniaxial compression tests were carried out for all specimens, and the mechanical properties were recorded.

Analysis of experimental results and corrosion mechanism

Porosity increment of specimens treated under different chemical conditions

Obviously, chemical corrosion of pore structures of sandstone is time-dependent, reflecting the kinetics of the chemical reaction between active minerals in sandstone and ions in the solution. The average porosity of specimens treated in different solutions against time are shown in Fig. 1. Clearly, porosity increases in all cases with time, indicating the occurrence of mineral dissolutions in these cases. For distilled water, any significant increment only happens in the first 20 days and little increase is observed afterwards. Acidic solution produces the highest corrosion in this case followed by the alkaline one. For both cases, as expected, the mineral dissolutions occurred quickly initially and then gradually slowed down until after 40 days when little changes in porosity was observed.

Mechanical property deterioration of sandstones

Typical uniaxial compressive stress–strain curves of the sandstone specimens tested are shown in Fig. 2. It can be seen that,

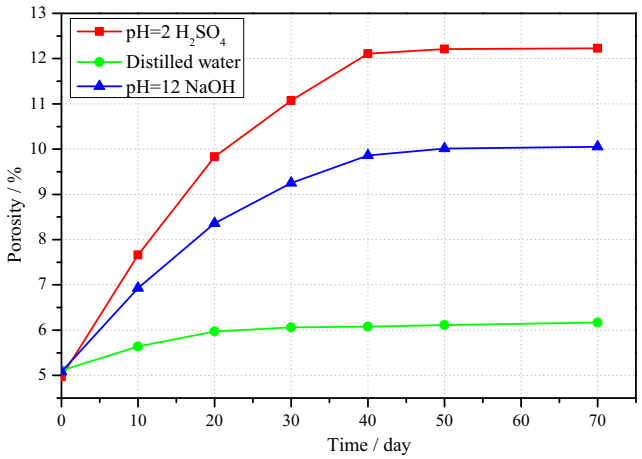

Fig. 1 Porosity variation under the effects of chemical environments

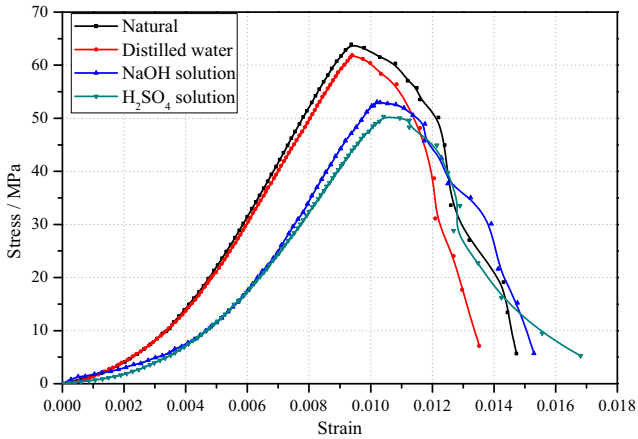

Fig. 2 Stress–strain curves of the sandstone specimens subjected to different chemical solutions

compared with the natural state sandstone, the peak strains of specimens treated in different solutions increased by different values. The result indicates that the chemical corrosion increases the plasticity of the rock. The common three main stages can also be observed in the stress–strain curves: (1) the stage of initial compaction, where the existing microcracks and micro-pores are compacted under the external load and the axial strain develops relatively quickly; (2) the stage of quasi-linear elasticity, where the stress–strain behavior is approximately linear, and the slope is used as the elastic modulus of sandstone in this work; (3) and the post-failure stage. As expected, corrosion causes the sandstone to become weaker, represented by smaller peak load and smaller elastic modulus. Moreover, the compaction stage is more obvious when the sandstone specimens are treated with chemical corrosion. In the post-failure stage, there were no significant differences among the stress–strain curves of the sandstones treated in different chemically corrosive solutions.

Table 1 lists the UCS, elastic modulus and peak strain of the specimens tested. Figure 3 shows the variety of the three mechanical properties for sandstone specimens after chemical corrosion. Compared with the natural-state sandstone, the UCS decreases by 2.69, 16.35 and 19.29% and the elastic modulus decreases by 6.29, 15.4 and 18.57% for specimens treated in distilled water, alkaline solution and acidic solution, respectively. These reductions are considered significant and are regarded as having serious impact on the stability of practical rock engineering applications. Moreover, the peak strain increased by 1.83, 8.83 and 12.07%, respectively, which indicates that the chemical corrosion can enhance the plasticity of the sandstone.

Moreover, the change rates of the mechanical properties for the sandstones immersed in NaOH or H_2SO_4 solutions are larger than that in distilled water, denoting that the order of the effect of chemical solutions on the sandstones is: H_2SO_4 solution > NaOH solution > distilled water.

Table 1 Uniaxial compression test results for specimens with different chemical solutions

Specimen group	Number	UCS (MPa)		Peak strain (10^{-3})		Elastic modulus (MPa)	
		Tested	Average	Tested	Average	Tested	Average
H_2SO_4	A1	50.32	51.06	10.62	10.40	8240	8283
	A2	52.28		10.42		8350	
	A3	50.58		10.18		8260	
Distilled water	B1	61.24	61.56	9.66	9.45	9430	9533
	B2	62.07		9.4		9620	
	B3	61.37		9.31		9550	
NaOH	C1	52.09	52.92	10.38	10.10	8470	8606
	C2	53.58		10.01		8560	
	C3	53.09		9.89		8790	
Natural	D1	63.91	63.26	9.32	9.28	9860	10,173
	D2	64.27		9.12		10,520	
	D3	61.60		9.41		10,140	

Chemical damage variable

The deterioration of mechanical properties of rock due to chemical corrosion, however, is the result of the combination of mechanical and corrosion damages. Therefore, it is necessary to introduce a chemical damage variable D_c to describe the damage caused by chemical corrosions.

In general, a damage variable can be defined using a certain property depending on application (Xu et al. 2017); i.e.,

$$D = 1 - \frac{f_n}{f_0} \tag{1}$$

where f_n is the property of rock after damage and f_0 is the property at a natural state. The property can be maximum strain, residual strain, elastic modulus, etc. However, it is inconvenient to obtain the mechanical properties by series of mechanical tests. Thus, other parameters have also been utilized to define the damage variable, such as porosity (Han et al. 2016; Li et al. 2018; Miao et al. 2018; Ni et al. 2016), computed tomography (CT) number (Peng et al. 2011; Teng et al. 2018; Wang et al. 2014) and rock density (Xiao et al. 2010). In this study, the chemical damage variable was calculated based on the porosity of sandstone specimens obtained by NMR.

When the porosity was utilized to define the chemical damage variable, the definition shown in Eq. (2) was most widely used (Han et al. 2016; Li et al. 2018; Ni et al. 2016). Note that porosity refers to the ratio of the sum of all pore space volumes in a rock sample to the volume of the rock sample. However, the damage variable is the irreversible change of the mesostructure in the material under the influence of external factors. It is described as the field of damage evolution in the macroscopic view. The specific physical meaning is the ratio of the effective bearing area of the micro-unit in the damaged state to the effective bearing area of the micro-unit in the non-destructive state. Therefore, it is not accurate to describe the chemical damage variable using Eq. (2).

$$D = \frac{\varnothing_t - \varnothing_0}{1 - \varnothing_0} \tag{2}$$

where $\varnothing_t$ is the porosity of sandstone specimens treated with chemical corrosion, and $_0$ is the initial porosity of the sandstone specimen.

Based on the principle of strain equivalence, Li et al. (2003) defined the chemical damage variable of sandstones after chemical corrosions based on the effective load-bearing area of the sandstone, i.e.:

$$D_c = \frac{\Delta S}{S_0} = \left(\frac{\Delta V}{V_0}\right)^{\frac{2}{3}} \tag{3}$$

where D_c is the chemical damage variable, ΔS and S_0 are the variety of the effective bearing area and the initial effective bearing area, respectively; ΔV and V_0 are the variety of the effective bearing volume and the initial effective bearing volume, respectively.

Studies by Lu et al. (2014) suggest that the chemical damage variable of rocks in Eq. (3) can be expressed in terms of porosity. Assuming that the volume of sandstone specimen is V, then we have:

$$\begin{cases} V'' = \varnothing_t \times V \\ V' = \varnothing_0 \times V \\ \Delta V = V'' - V' \\ V_0 = V - V' \end{cases} \tag{4}$$

where V'' and V' are the effective bearing volume of sandstone specimens at the damage state and the initial state, respectively.

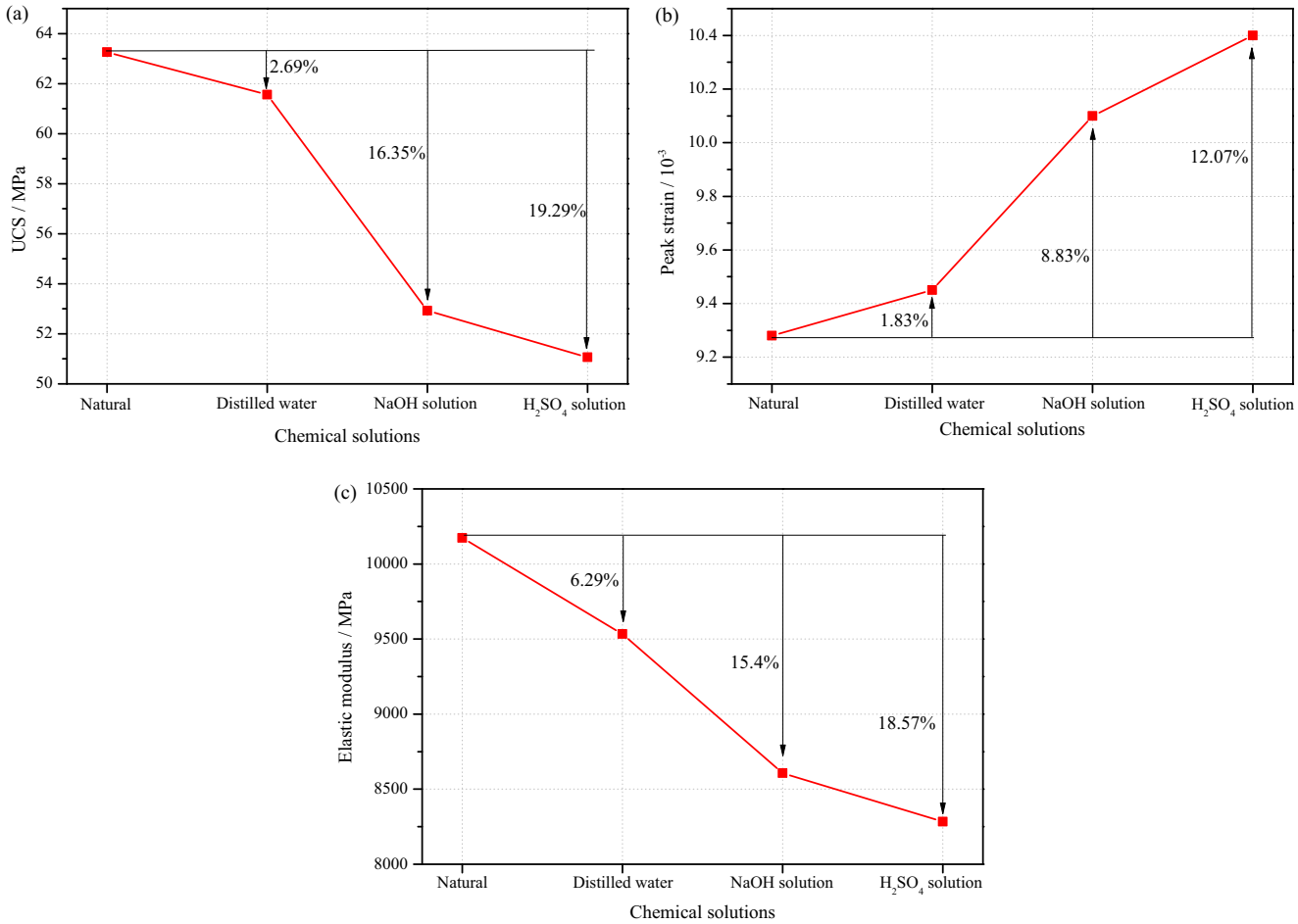

Fig. 3 Variety of mechanical properties for sandstone specimens subjected to different chemical solutions. (**a**) UCS; (**b**) peak strain; (**c**) elastic modulus

Combining Eqs. (3) and (4), the chemical damage variable can be obtained:

$$D_c = \left(\frac{\varnothing_t - \varnothing_0}{1 - \varnothing_0}\right)^{\frac{2}{3}} \tag{5}$$

In this work, the chemical damage variable is calculated by Eq. (5). The chemical damage of the sandstone specimens immersed in different chemical solutions are shown in Fig. 4. After being soaked in distilled water, NaOH solution and H_2SO_4 solution, the values of chemical damage variables are 0.05, 0.14 and 0.18, respectively. Compared with the natural-state sandstone, the chemical damage increases in varying degrees, and the increment of the sandstones treated in NaOH or H_2SO_4 solutions are more significant. The order of the chemical damage variables is: $D_{H2SO4} > D_{NaOH} > D_{distilled\ water}$, which is consistent with the change rates of mechanical properties of the sandstones treated in different chemical solutions. Both of these suggest that the corrosion effect of H_2SO_4 solution on the sandstones is the largest, followed by NaOH solution and distilled water, respectively.

Analysis of the corrosion mechanism

Natural rocks are formed by cemented mineral compounds and internal defects such as pores and micro-cracks (Gao et al. 2016). In the presence of chemical solution, fluid will penetrate into pores and cracks and interact with minerals through dissolution and chemical reactions. These corrosion processes cause microscopic structural damage within the rock, resulting in the deterioration of rock mechanical properties (Fang et al. 2018).

Due to different minerals contained in different rocks, the reaction between rock and different chemical solutions will also be different. As discussed above, the main minerals of sandstones used in the study are quartz (75%), feldspar (12%), mica (7%), calcite (3%) and chlorite (2%). As quartz, feldspar and mica together account for 94% of the total mineral composition, their reactions with the chemical solution will play the key role in the porosity change and deterioration of mechanical properties.

When immersed in chemical solutions, minerals such as quartz, feldspar and mica can easily react with the hydrogen ion (H^+) and hydroxyl ion (OH^-). Minerals such as calcite are

soluble in water. The key corrosion mechanisms for the sandstone studied in this work are summarized below.

In distilled water, the dissolution equation of quartz in water is

$$SiO_2 + 2H_2O \rightarrow H_4SiO_4 \tag{6}$$

In addition, the following reactions may occur due to the presence of clay minerals within the sandstone. These are termed secondary reactions:

$$\begin{cases} CaO + H_2O \rightarrow Ca(OH)_2 \\ MgO + H_2O \rightarrow Mg(OH)_2 \\ K_2O + H_2O \rightarrow 2K^+ + 2OH^- \end{cases} \tag{7}$$

In acidic solution (H_2SO_4), there are three main reactions related to quartz, feldspar and mica minerals, i.e.,:

$$\begin{cases} SiO_2 + 4H^+ \rightarrow Si^{4+} + 2H_2O \\ KAlSi_3O_8 + 4H^+ + 4H_2O \rightarrow Al^{3+} + K^+ + 3H_4SiO_4 \\ KAl_3Si_3O_{10}(OH)_2 + 10H^+ \rightarrow 3Al^{3+} + K^+ + 3H_4SiO_4 \end{cases} \tag{8}$$

In addition, the following reactions may also occur due to the presence of calcite, chlorite and clay minerals (Pearce et al. 2015; Yuan et al. 2017):

$$\begin{cases} CaCO_3 + 2H^+ \rightarrow Ca^{2+} + H_2O + CO_2\uparrow \\ CaO + 2H^+ \rightarrow Ca^{2+} + H_2O \\ Fe_2O_3 + 6H^+ \rightarrow 2Fe^{3+} + 3H_2O \\ Fe_4MgAl_2Si_3O_{10}(OH)_8 + 10H^+ \rightarrow 4Fe^{2+} + Mg^{2+} + Al_2Si_2O_5(OH)_4 + SiO_2 + 7H_2O \end{cases} \tag{9}$$

Note that the reaction between calcite and hydrogen ion (H^+) is an exothermic reaction, which will then indirectly increase the chemical corrosion effect. In alkaline solution (NaOH), the three main reactions are:

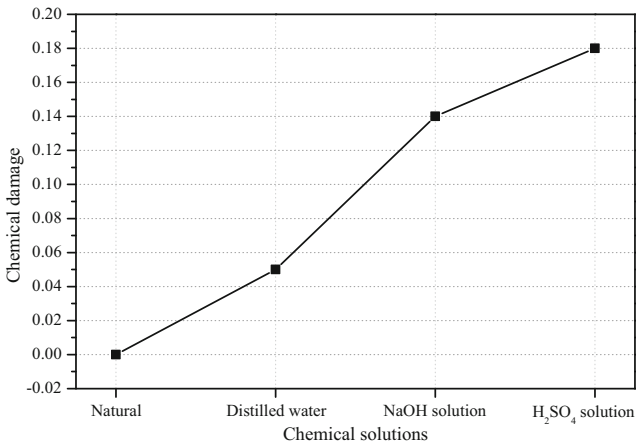

Fig. 4 Variety of chemical damage variables of the sandstones subjected to different chemical solutions

$$\begin{cases} SiO_2 + 2OH^- \rightarrow SiO_3^{2-} + H_2O \\ KAlSi_3O_8 + 6OH^- + 2H_2O \rightarrow 3H_2SiO_4^{2-} + K^+ + Al(OH)_4^- \\ KAl_3Si_3O_{10}(OH)_2 + H_2O + 8OH^- \rightarrow 3SiO_3{}^{2-} + K^+ + 3Al(OH)_4^- \end{cases} \tag{10}$$

In this case, all major minerals (quartz, feldspar and mica) are involved in the reactions. However, the reaction between quartz and OH^- produces insoluble deposits. Therefore, the chemical corrosion effect of alkaline solutions is less severe compared with that of acidic solutions for the sandstone studied.

In both acidic and alkaline solutions, the dissolutions described in Eq. (6) and (7) can also occur. The corrosion caused by the dissolutions is less significant compared with the chemical reactions described above, which will play the key role for the corrosions, leading to the significant changes in porosity and mechanical properties.

Damage constitutive model due to chemical corrosions

Damage constitutive relationship of sandstone after chemical corrosion

According to the equivalent strain hypothesis (Lemaitre 1985) and the theory of continuum damage mechanics (Chen et al. 2018), the damage constitutive relationship of rock is:

$$\begin{cases} \sigma' = \dfrac{\sigma}{1-D} \\ \sigma = (1-D)E\varepsilon \end{cases} \tag{11}$$

where σ is the nominal stress, σ' is the effective stress, D is the total damage variable, and E and ε are the elastic modulus and strain of rock, respectively.

Under the condition of uniaxial compression, the damage constitutive relationship of rock without chemical corrosion can be described as:

$$\sigma = (1-D_m)E\varepsilon \tag{12}$$

where D_m is the damage variable of rock caused by a load.

Conceptually, a rock can be divided into a number of micro-elements. The ratio of the number of failed micro-elements N_t to the total number of micro-elements N can then be used to define the accumulation effect of the element destruction during rock loading (the damage variable, D_m), i.e.,

$$D_m = \frac{N_t}{N} \tag{13}$$

In this conceptual approach, these micro-elements have different strength and the weakest element will fail first. It is natural to assume these element strengths are different due to rock heterogeneity and follow a certain statistical distribution,

with the most commonly used in damage mechanics as the Weibull distribution (Weibull 1951). Therefore, it is appropriate to use the Weibull function in a constitutive model to reflect the statistical distribution of strength in rocks.

For a Weibull distribution, the probability density function $p(F)$ of the strength of micro-elements can be expressed as:

$$p(F) = \frac{m}{F_0}\left(\frac{F}{F_0}\right)^{m-1} e^{-\left(\frac{F}{F_0}\right)^m} \tag{14}$$

where m and F_0 are the Weibull distribution parameters of rocks, F is the random variable of Weibull distribution, which, in this case, is the strength of micro-elements.

Then the damage variable D_m can be obtained at the stress level F:

$$\begin{aligned} D_m &= \int_0^F p(F)dF = \int_0^F \frac{m}{F_0}\left(\frac{F}{F_0}\right)^{m-1} e^{-\left(\frac{F}{F_0}\right)^m} dF \\ &= 1-e^{-\left(\frac{F}{F_0}\right)^m} \end{aligned} \tag{15}$$

Substituting Eq. (15) into Eq. (12) leads to

$$\sigma = E\varepsilon e^{-\left(\frac{F}{F_0}\right)^m} \tag{16}$$

As can be seen in Section 3, the damage characteristics of the sandstones treated with different chemical corrosions are different. However, the damage variable D_m in Eq. (15) is the damage caused by the load, and the damage behavior of the sandstone after chemical corrosion is caused by the combination of chemical corrosion and load. Therefore, the constitutive model in Eq. (16) cannot fully describe the mechanical behavior of rock after chemical corrosion. This also addresses a need to establish a more reasonable constitutive model of rock under the coupling effect of chemical corrosion and load.

As a description of the generalized equivalent strain principle (Qu et al. 2018), the initial damage state of rock is defined as the baseline damage state, and the rock is damaged under the action of load. Taking any two of these damage states, and then the strain, which is caused by the effective stress of the rock in the first damage state on the rock in the second damage state, is equivalent to the strain caused by the effective stress of the rock in the second damage state on the rock in first damage state. The assumption can be written as:

$$\varepsilon = \frac{\sigma^1}{E^2} = \frac{\sigma^2}{E^1} \tag{17}$$

where $\sigma^1$and σ^2 are the effective stress of the rock in the first and second damage state, respectively. $E^1$and $E^2$are the elastic modulus of the rock in the first and second damage state, respectively.

Assuming that the baseline damage state of the sandstone is the first damage state, and the chemical corrosion damage state is the second damage state, then we have:

$$\varepsilon = \frac{\sigma_0}{E_c} = \frac{\sigma_c}{E_0} \tag{18}$$

where σ_0 and σ_c are the effective stress of the rock in the baseline and chemical damage state, respectively. E_0 and E_c are the elastic modulus of the rock in the baseline and chemical damage state, respectively.

According to Eq. (11), we have:

$$\sigma_c = \frac{\sigma_0}{(1-D_c)} \tag{19}$$

Combining Eqs. (18) and (19), the elastic modulus of the sandstone treated with chemical corrosion can be obtained as (Miao et al. 2018):

$$E_c = E_0(1-D_c) \tag{20}$$

where E_c is the elastic modulus of sandstones treated with chemical corrosion, and E_0 is the initial elastic modulus.

Similarly, considering the chemical corrosion damage state as the first damage state, and the damage state of the coupling chemical corrosion and load as the second damage state, then the constitutive relationship of rock under the coupling effect of chemical corrosion and load is:

$$\sigma = E_c(1-D_m)\varepsilon \tag{21}$$

Combining Eqs. (20) and (21), the constitutive model of rock can be written as:

$$\sigma = E_0(1-D)\varepsilon \tag{22}$$

where the total damage variable $D = D_c + D_m - D_cD_m$.

Substituting Eq. (15) into Eq. (22), the damage constitutive model of sandstones after chemical corrosion under uniaxial compression is:

$$\sigma = (1-D)E_0\varepsilon = (1-D_c)E_0\varepsilon\, e^{-\left(\frac{F}{F_0}\right)^m} \tag{23}$$

Let $E = (1 - D_c)E_0$, then Eq. (23) can be written as

$$\sigma = E\varepsilon\, e^{-\left(\frac{F}{F_0}\right)^m} \tag{24}$$

Determination of m and F_0

It is necessary to use a reasonable failure criterion to describe the strength of micro-elements (the random variable of Weibull distribution) in the damage constitutive model (Xu and Karakus 2018). The criterions of Drucker–Prager (D–P), Mohr–Coulomb and Hoek–Brown have been widely used in

previous researches. The D–P criterion, which has been successfully used (Deng and Gu 2011; Li et al. 2012), is proposed for the constitutive model in this study. The D–P criterion can be expressed as:

$$F = \alpha_0 I_1 + \sqrt{J_2} = k_0 \tag{25}$$

where α_0 is a constant related to the cohesion and internal friction angle of the rock, I_1 and J_2 are the first invariant of the stress tensor and the second invariant of the stress deviator, respectively, which are given as:

$$\begin{cases} I_1 = \sigma_1' + \sigma_2' + \sigma_3' \\ J_2 = \dfrac{(\sigma_1'-\sigma_2')^2 + (\sigma_2'-\sigma_3')^2 + (\sigma_3'-\sigma_1')^2}{6} \end{cases} \tag{26}$$

where $\sigma_1', \sigma_2', \sigma_3'$ are effective stresses.

According to the assumption of equivalent strain of Lemaitre, it can be seen that the effective stress of rock can be represented by the nominal stress, that is:

$$\begin{cases} \sigma_1' = \sigma_1/(1-D_m) \\ \sigma_2' = \sigma_2/(1-D_m) \\ \sigma_3' = \sigma_3/(1-D_m) \end{cases} \tag{27}$$

Assuming that the deformation of rocks follows the linear elastic Hooke's law, we have:

$$\sigma_1' = E\varepsilon_1 + \mu\left(\sigma_2' + \sigma_3'\right) \tag{28}$$

Substituting Eq. (27) into Eq. (28) leads to:

$$1-D_m = \frac{\sigma_1 - \mu(\sigma_2 + \sigma_3)}{E\varepsilon_1} \tag{29}$$

Combining Eqs. (25) ~ (29), the strength F of micro-elements can be expressed as:

$$F = \frac{\left(\alpha_0 I_1' + \sqrt{J_2'}\right) E\varepsilon_1}{\sigma_1 - \mu(\sigma_2 + \sigma_3)} \tag{30}$$

where $I_1' = \sigma_1 + \sigma_2 + \sigma_3$, $J_2' = \frac{(\sigma_1-\sigma_2)^2+(\sigma_2-\sigma_3)^2+(\sigma_3-\sigma_1)^2}{6}$.

Under uniaxial loading condition, $\sigma = \sigma_1$, $\sigma_2 = \sigma_3 = 0$ and $\varepsilon = \varepsilon_1$, the strength of micro-element F can be written as:

$$F = \left(\alpha_0 + \frac{\sqrt{3}}{3}\right) E\varepsilon \tag{31}$$

Substituting Eq. (31) into Eq. (24), the expression of the damage constitutive model of rocks can be written as:

$$\sigma = E\varepsilon e^{-\left[\frac{\left(\alpha_0+\frac{\sqrt{3}}{3}\right)E\varepsilon}{F_0}\right]^m} \tag{32}$$

For the stress–strain curve of rocks, the peak load point (P) in theory should satisfy the following relationships:

$$\begin{cases} \sigma = \sigma_p \\ \varepsilon = \varepsilon_p \\ \dfrac{d\sigma}{d\varepsilon} = 0 \end{cases} \tag{33}$$

where σ_p and ε_p are the stress and strain at the peak point, respectively.

Differentiating Eq. (32), the following expression can be obtained:

$$\frac{d\sigma}{d\varepsilon} = Ee^{-\left[\frac{\left(\alpha_0+\frac{\sqrt{3}}{3}\right)E\varepsilon}{F_0}\right]^m} - \frac{\alpha_0 + \frac{\sqrt{3}}{3}}{F_0} mE^{m+1}\varepsilon^m e^{-\left[\frac{\left(\alpha_0+\frac{\sqrt{3}}{3}\right)E\varepsilon}{F_0}\right]^m} \tag{34}$$

Substituting Eq. (23) into Eqs. (34) and (32), we have

$$\begin{cases} \left[\dfrac{\left(\alpha_0 + \frac{\sqrt{3}}{3}\right)E\varepsilon_p}{F_0}\right]^m = \dfrac{1}{m} \\ ln\dfrac{E\varepsilon_p}{\sigma_p} = \left[\dfrac{\left(\alpha_0 + \frac{\sqrt{3}}{3}\right)E\varepsilon_p}{F_0}\right]^m \end{cases} \tag{35}$$

Then, solving Eq. (35), we have

$$\begin{cases} m = \dfrac{1}{ln\dfrac{E\varepsilon_p}{\sigma_p}} \\ F_0 = \left(\alpha_0 + \dfrac{\sqrt{3}}{3}\right) E\varepsilon_p m^{\frac{1}{m}} \end{cases} \tag{36}$$

Substituting Eq. (36) into (32), the damage evolution relationship and constitutive model can be written as:

$$\sigma = E\varepsilon e^{-\frac{1}{m}\left(\frac{\varepsilon}{\varepsilon_p}\right)^m} = (1-D_c)E_0\varepsilon e^{-\frac{1}{m}\left(\frac{\varepsilon}{\varepsilon_p}\right)^m} \tag{37}$$

According to the results shown in Section 3.2, the uniaxial compressive stress–strain curve of the sandstone can be divided into three stages. Note that the stress–stain curves at the stages of compaction and quasi-linear elasticity are concave, and the slope of the stress–strain curve increases logarithmically with the strain. Therefore, the damage constitutive model in Eq. (37) does not reflect the characteristic of pore compaction under load. Thus, the model needs to be modified. According to previous researches (Liu et al. 2016; Liu et al. 2018; Xu et al. 2017), the compaction coefficient K, defined as the ratio of the slope of the stress–strain curve to the elastic modulus E, can well describe the compaction characteristics of rock material. The coefficient can be used to modify the slope of the curves, and can be evaluated as (Liu et al. 2016):

Table 2 Parameters of the damage model of sandstone under the conditions of different chemical corrosion

Chemical solutions	σ_p /Mpa	ε_p /10^{-3}	m	D_c	E_0 / GPa	n
H_2SO_4 (A)	51.06	10.40	2.03	0.18	10.17	0.3475
Distilled water (B)	61.56	9.45	2.65	0.05	10.17	0.7143
NaOH (C)	52.92	10.10	1.91	0.14	10.17	0.2652
Natural (D)	63.26	9.28	2.61	0	10.17	0.6311

$$K = \begin{cases} log_n\left(\frac{n-1}{\varepsilon_s}\varepsilon + 1\right) & \varepsilon \le \varepsilon_s \\ 1 & \varepsilon > \varepsilon_s \end{cases} \tag{38}$$

where n is a constant obtained experimentally, and ε_s is the strain corresponding to the yield stress. In this study, the compaction coefficient was introduced and the constitutive model can be modified as:

$$\sigma = KE\varepsilon e^{-\left(\frac{F}{F_0}\right)^m} = K(1-D_c)E_0\varepsilon e^{-\frac{1}{m}\left(\frac{\varepsilon}{\varepsilon_p}\right)^m} \tag{39}$$

When the compaction characteristics coefficient was not considered, the constitutive model can be written as Eq. (40), which has been widely used in many literatures (Jiang and Wen 2011; Miao et al. 2018).

$$\sigma = (1-D_c)E_0\varepsilon e^{-\frac{1}{m}\left(\frac{\varepsilon}{\varepsilon_p}\right)^m} \tag{40}$$

Verification of statistical damage constitutive model

The experimental results of the groups A1~A3, B1~B3, C1~C3 and D1~D3 are used to calibrate the parameters for the damage constitutive model of sandstones treated with different chemical corrosions and the results are shown in Table 2. In Table 2, σ_p and ε_p are the stress and strain at the peak point on the stress–strain curve. The parameter m is calculated based on Eq. (36). The chemical damage variable D_c is calculated based on Eq. (5). The constant n can be obtained from the results of loading tests using a least squares regression (Liu et al. 2016). The model is then validated on the data from the remaining samples of A3, B3, C3 and D3 to

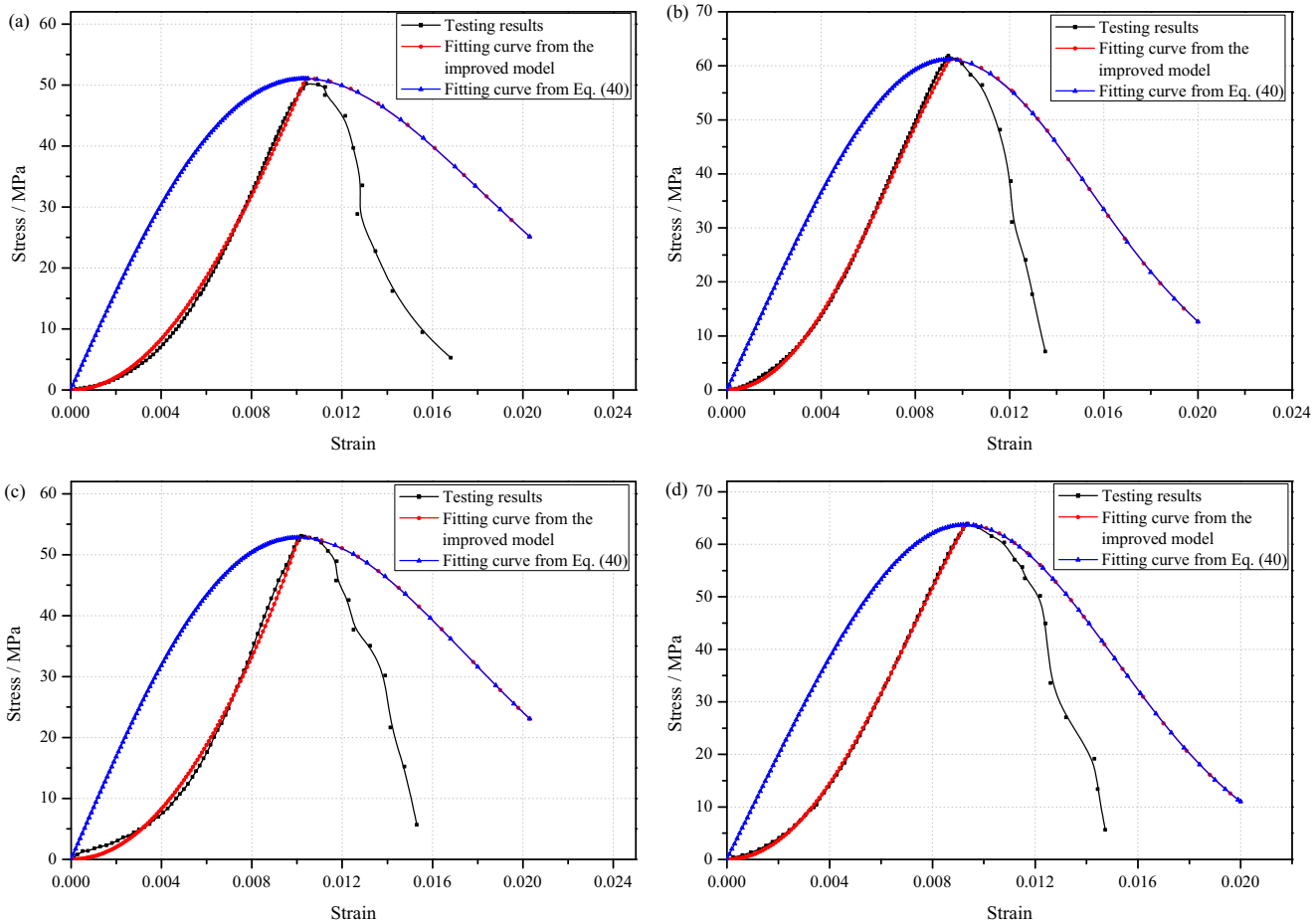

Fig. 5 Test results and theoretical curves of sandstone specimens treated with different chemical corrosion. The chemical solutions are: (**a**) H_2SO_4 solution; (**b**) distilled water; (**c**) NaOH solution; (**d**) natural

assess the reliability of the proposed constitutive model. For comparison, the constitutive model shown in Eq. (40) which did not consider the compaction characteristics of the stress–strain curves is also displayed.

The simulation results are shown in Fig. 5. It can be seen that the improved damage constitutive model proposed in this study can describe the basic characteristics of mechanical properties of sandstone treated with chemical corrosion under the uniaxial loading. Especially in the stage before peak stress, the simulation results are very similar to the experimental data, and can objectively characterize the constitutive relationship of sandstone before peak stress. Compared with the simulation results of the improved model and the model without the compaction coefficient, it can be found that the simulation results of the model without the compaction coefficient deviate greatly from the experimental data. Meanwhile, the improved model proposed in this study has a better fitting effect on the mechanical properties of sandstone treated with chemical corrosion, and can better reveal the closure-initiation-development process of micro-cracks inside the rock.

In the post-peak stress stage, there is a certain deviation between the simulated curves and the experimental curves. This may be due to the theoretical model being established based on the theory of meso-statistical damage mechanics, which is mainly used to study the evolution of macro-cracks inside the rocks. However, the characteristics of the post-peak stage is mainly the extension of macro-cracks. Since the proposed model did not consider the behavior characteristics of these factors, then the deviation is generated. Moreover, the obtained information on the stress–strain curves may be inaccurate after the peak strength has passed, which then results in the increase of errors.

On the whole, the closure-initiation-development process of micro-cracks inside the sandstone can be better fitted by the improved constitutive model proposed in this study. In addition, the mechanical properties, such as the peak stress, peak strain and the elastic modulus, are highly consistent with that of the test data. Therefore, the damage constitutive model of sandstone under load in a chemical environment is basically in line with the actual conditions. Note that the focus of the study is the damage evolution and constitutive model of rock under the state of uniaxial compression. Research on the mechanical properties and constitutive model of rock under triaxial compression will be further work.

Conclusions

In this study, the damage evolution and constitutive model of sandstones with different chemical corrosion were investigated through NMR technology and UCS testing. The following conclusions can be drawn based on the results obtained in this study:

(1) Compared with the natural specimen, the porosity of sandstone specimens with chemical corrosion increases. Based on the change of porosity of sandstone with chemical corrosion, the chemical damage variable is established. For sandstone soaked in distilled water, NaOH solution and H_2SO_4 solution, the values of chemical damage variables are 0.05, 0.14 and 0.18, respectively. The order of chemical damage variable is: $D_{H2SO4} > D_{NaOH} > D_{\text{distilled water}}$.

(2) Compared with the natural specimen, mechanical properties of sandstone with different chemical corrosion deteriorate. Compared with the natural-state sandstone, the UCS decreases by 2.69, 16.35 and 19.29%, the elastic modulus decreases by 6.29, 15.4 and 18.57%, while the peak strain increases 1.83, 8.83 and 12.07% for specimens treated in distilled water, alkaline solution and acidic solution, respectively. Corrosion of chemical solutions results in the decrease in strength and the increase in ductility of the sandstone. The effect order of chemical solution on mechanical properties of sandstone is: H_2SO_4 > NaOH > distilled water.

(3) The chemical reactions are different with the variation of chemical solutions. The mineral compositions are more active in H_2SO_4 solution, and the reactions between quartz, feldspar, mica and chemical solutions are the main factors which affect the pore structure of sandstone specimens.

(4) An improved statistical damage constitutive model by combining the compaction coefficient and the chemical damage variable is proposed to describe the damage evolution of sandstones treated with chemical corrosion. Based on experimental data, the proposed model is verified to be able to describe satisfactorily the deterioration in mechanical properties of sandstone with different chemical corrosion.

Acknowledgments The research presented in this paper was jointly supported by the National Natural Science Foundation of China (grant no. 51774323 and no. 41502327), the Fundamental Research Funds Project for the Central South University (grant no.2016zzts095), and the Open-End Fund for the Valuable and Precision Instruments of Central South University (grant no. CSUZC201801). The first author would like to thank the Chinese Scholarship Council for financial support to the joint PhD studies at the University of Adelaide.

References

Bieniawski Z, Bernede M (1979) Suggested methods for determining the uniaxial compressive strength and deformability of rock materials: part 1. Suggested method for determination of the uniaxial compressive strength of rock materials. Int J Rock Mech Min Geomech Abstr 16(2):138–140

Chaki S, Takarli M, Agbodjan WP (2008) Influence of thermal damage on physical properties of a granite rock: porosity, permeability and

ultrasonic wave evolutions. Constr Bulid Mater 22:1456–1461. https://doi.org/10.1016/j.conbuildmat.2007.04.002

Chen S, Qiao C, Ye Q, Khan MU (2018) Comparative study on three-dimensional statistical damage constitutive modified model of rock based on power function and Weibull distribution. Environ Earth Sci 77:108. https://doi.org/10.1007/s12665-018-7297-6

Darabi MK, Abu Al-Rub RK, Little DN (2012) A continuum damage mechanics framework for modeling micro-damage healing. Int J Solids Struct 49:492–513. https://doi.org/10.1016/j.ijsolstr.2011.10.017

Deng J, Gu D (2011) On a statistical damage constitutive model for rock materials. Comput Geosci 37:122–128. https://doi.org/10.1016/j.cageo.2010.05.018

Fang X, Xu J, Wang P (2018) Compressive failure characteristics of yellow sandstone subjected to the coupling effects of chemical corrosion and repeated freezing and thawing. Eng Geol 233:160–171. https://doi.org/10.1016/j.enggeo.2017.12.014

Feng X, Chen S, Zhou H (2004) Real-time computerized tomography (CT) experiments on sandstone damage evolution during triaxial compression with chemical corrosion. Int. J. Rock Mech. Min. 41:181–192. https://doi.org/10.1016/s1365-1609(03)00059-5

Gao F, Wang Q, Deng H, Zhang J, Tian W, Ke B (2016) Coupled effects of chemical environments and freeze–thaw cycles on damage characteristics of red sandstone. B. Eng. Geol. Environ. 76:1481–1490. https://doi.org/10.1007/s10064-016-0908-0

Han T, Shi J, Cao X (2016) Fracturing and damage to sandstone under coupling effects of chemical corrosion and freeze–thaw cycles. Rock Mech Rock Eng 49:4245–4255. https://doi.org/10.1007/s00603-016-1028-7

Han T, Shi J, Chen Y, Li Z, Li C (2017) Laboratory investigation on the mechanical properties of sandstone immersed in different chemical corrosion under freeze-thaw cycles. Acta Mech. Solida Sin.:503–520

Hu D, Zhou H, Hu Q, Shao J, Feng X, Xiao H (2012) A hydro-mechanical-chemical coupling model for geomaterial with both mechanical and chemical damages considered. Acta Mech Solida Sin 25:361–376. https://doi.org/10.1016/s0894-9166(12)60033-0

Jiang L, Wen Y (2011) Damage constitutive model of sandstone during corrosion by AMD. J Cent South Univ 42:3502–3506 **(in Chinese)**

Lemaitre J (1985) A continuous damage mechanics model for ductile fracture. J Eng Mater Technol 107:83–89. https://doi.org/10.1115/1.3225775

Li G, Tang C-A (2015) A statistical meso-damage mechanical method for modeling trans-scale progressive failure process of rock. Int. J. Rock Mech. Min. 74:133–150. https://doi.org/10.1016/j.ijrmms.2014.12.006

Li H, Xiong G, Zhao G (2016a) An elasto-plastic constitutive model for soft rock considering mobilization of strength. T Nonferr Metal Soc 26:822–834. https://doi.org/10.1016/s1003-6326(16)64173-0

Li H, Yang D, Zhong Z, Sheng Y, Liu X (2018) Experimental investigation on the micro damage evolution of chemical corroded limestone subjected to cyclic loads. Int J Fatigue 113:23–32. https://doi.org/10.1016/j.ijfatigue.2018.03.022

Li J, Zhou K, Liu W, Deng H (2016b) NMR research on deterioration characteristics of microscopic structure of sandstones in freeze–thaw cycles. T. Nonferr. Metal. Soc. 26:2997–3003. https://doi.org/10.1016/s1003-6326(16)64430-8

Li N, Zhu Y, Su B, S. G (2003) A chemical damage model of sandstone in acid solution. Int J Rock Mech Min 40:243–249. https://doi.org/10.1016/s1365-1609(02)00132-6

Li X, Cao W, Su Y (2012) A statistical damage constitutive model for softening behavior of rocks. Eng Geol 143-144:1–17. https://doi.org/10.1016/j.enggeo.2012.05.005

Liu C, Deng H, Wang Y, Lin Y, Zhao H (2017) Time-varying characteristics of granite microstructures after cyclic dynamic disturbance using nuclear magnetic resonance. Crystals 7:306–317. https://doi.org/10.3390/cryst7100306

Liu X, Ning J, Tan Y, Gu Q (2016) Damage constitutive model based on energy dissipation for intact rock subjected to cyclic loading. Int. J. Rock Mech. Min. 85:27–32. https://doi.org/10.1016/j.ijrmms.2016.03.003

Liu X, Tan Y, Ning J, Lu Y, Gu Q (2018) Mechanical properties and damage constitutive model of coal in coal-rock combined body. Int. J. Rock Mech. Min. 110:140–150. https://doi.org/10.1016/j.ijrmms.2018.07.020

Lu G, Yan E, Wang X, Xie L, Gao L (2014) Study of impact of fractal dimension of pore distribution on compressive strength of porous material. Rock Soil Mech 35:2261–2269 **(in Chinese)**

Lu Y, Wang L, Sun X, Wang J (2016) Experimental study of the influence of water and temperature on the mechanical behavior of mudstone and sandstone. B Eng Geol Environ 76:645–660. https://doi.org/10.1007/s10064-016-0851-0

Miao S, Wang H, Cai M, Song Y, Ma J (2018) Damage constitutive model and variables of cracked rock in a hydro-chemical environment. Arab J Geosci 11:1–19. https://doi.org/10.1007/s12517-017-3373-6

Ni J, Chen Y, Wang P, Wang S, Peng B, Azzam R (2016) Effect of chemical erosion and freeze–thaw cycling on the physical and mechanical characteristics of granites. B. Eng. Geol. Environ. 76:169–179. https://doi.org/10.1007/s10064-016-0891-5

Pearce JK, Kirste DM, Dawson GKW, Farquhar SM, Biddle D, Golding SD, Rudolph V (2015) SO_2 impurity impacts on experimental and simulated CO_2 –water–reservoir rock reactions at carbon storage conditions. Chem Geol 399:65–86. https://doi.org/10.1016/j.chemgeo.2014.10.028

Peng R, Yang Y, Ju Y, Mao L, Yang Y (2011) Computation of fractal dimension of rock pores based on gray CT images. Chin Sci Bull 56:3346–3357. https://doi.org/10.1007/s11434-011-4683-9

Pourhosseini O, Shabanimashcool M (2014) Development of an elasto-plastic constitutive model for intact rocks. Int. J. Rock Mech. Min. 66:1–12. https://doi.org/10.1016/j.ijrmms.2013.11.010

Qiao L, Wang Z, Huang A (2016) Alteration of mesoscopic properties and mechanical behavior of sandstone due to hydro-physical and hydro-chemical effects. Rock Mech Rock Eng 50:255–267. https://doi.org/10.1007/s00603-016-1111-0

Qu D, Li D, Li X, Luo Y, Xu K (2018) Damage evolution mechanism and constitutive model of freeze- thaw yellow sandstone in acidic environment. Cold Reg Sci Technol 155:174–183. https://doi.org/10.1016/j.coldregions.2018.07.012

Tang L, Zhang P, Wang S (2002) Testing study on macroscopic mechanics effect of chemical action of water on rocks. Chinese J Rock Mech Eng 21:526–531

Teng J, Tang J, Zhang Y, Li X (2018) CT experimental study on the damage characteristics of anchored layered rocks. KSCE J Civ Eng:1–10. https://doi.org/10.1007/s12205-018-0425-8

Wang Y, Li X, Zhang B, Wu Y (2014) Meso-damage cracking characteristics analysis for rock and soil aggregate with CT test. Sci China Technol Sc 57:1361–1371. https://doi.org/10.1007/s11431-014-5578-1

Wang Z, Li Y, Wang JG (2007) A damage-softening statistical constitutive model considering rock residual strength. Comput Geosci 33:1–9. https://doi.org/10.1016/j.cageo.2006.02.011

Weibull W (1951) A statistical distribution function of wide applicability. J Appl Mech 18:293–297

Xiao J, Ding D, Jiang F, Xu G (2010) Fatigue damage variable and evolution of rock subjected to cyclic loading. Int J Rock Mech Min 47:461–468. https://doi.org/10.1016/j.ijrmms.2009.11.003

Xu X, Gao F, Zhang Z (2017) Thermo-mechanical coupling damage constitutive model of rock based on the Hoek–Brown strength criterion. Int J Damage Mech:105678951772683. https://doi.org/10.1177/1056789517726838

Xu XL, Karakus M (2018) A coupled thermo-mechanical damage model for granite. Int. J. Rock Mech. Min. 103:195–204. https://doi.org/10.1016/j.ijrmms.2018.01.030

Yang X, Weng L, Hu Z (2017) Damage evolution of rocks under triaxial compressions: an NMR investigation. KSCE J Civ Eng 22(8):2856–2863. https://doi.org/10.1007/s12205-017-0766-8

Yuan W, Liu X, Fu Y (2017) Chemical thermodynamics and chemical kinetics analysis of sandstone dissolution under the action of dry–wet cycles in acid and alkaline environments. B. Eng. Geol. Environ. https://doi.org/10.1007/s10064-017-1162-9

Zhao H, Zhang C, Cao W, Zhao M (2016) Statistical meso-damage model for quasi-brittle rocks to account for damage tolerance principle. Environ Earth Sci 75. https://doi.org/10.1007/s12665-016-5681-7

Zhou K, Li B, Li J, Deng H, Bin F (2015) Microscopic damage and dynamic mechanical properties of rock under freeze–thaw environment. T. Nonferr. Metal. Soc. 25:1254–1261. https://doi.org/10.1016/s1003-6326(15)63723-2

Zhou K, Liu T, Hu Z (2018) Exploration of damage evolution in marble due to lateral unloading using nuclear magnetic resonance. Eng Geol 244:75–85

Zhou Z, Cai X, Cao W, Li X, Xiong C (2016) Influence of water content on mechanical properties of rock in both saturation and drying processes. Rock Mech Rock Eng 49:3009–3025. https://doi.org/10.1007/s00603-016-0987-z